https://doi.org/10.5194/egusphere-2026-3145
Preprint. Discussion started: 15 June 2026

Systematic valley floor extraction for characterizing valley width distribution in mountain landscapes : comparison between hydraulic and geometrical approaches

Aude Lurin[1], Philippe Steer[1], Fiona Clubb[2], and Boris Gailleton[1]

[1]Geosciences Rennes, Université de Rennes, Rennes, Fance
[2]Department of Geography, Durham University, Durham, UK

Correspondence: Aude Lurin (aude.lurin@univ-rennes.fr)

Abstract. Valleys are key elements of mountainous landscapes, governing the transfer of water and sediment while recording the influence of tectonic and climatic forcing. Despite their importance, the quantitative characterization of valley morphology at large spatial scales remains challenging, particularly due to limitations in automated extraction methods. In this study, we compare two approaches for delineating valley extent from digital elevation models: a classical geometrical method based on topographic thresholds, and a novel pseudo-hydraulic method that estimates flood-prone areas using a simplified water-filling algorithm. Using 30 m resolution DEMs, we find that both perform well and that the conceptual difference between them is mainly significant in headwater areas. We then find that the main control on valley width is drainage area, consistent with previous work. The use of a wideness index allows us to identify local deviations from the width–area scaling, highlighting secondary controls such as lithological changes. New insights into valley morphology could be obtained through the large-scale systematic extraction of valleys across various tectonic and climatic settings.

1 Introduction

Valleys are fundamental components of mountain landscape dynamics, acting as conveyors of sediments and water while transmitting tectonic and climatic signals across landscapes (Amos and Burbank, 2007; Hancock and Anderson, 2002; Fisher et al., 2013). They are often densely populated and cultivated areas (Cooper et al., 2003; Thorp et al., 2006; Felipe-Lucia et al., 2014; Tomscha et al., 2017), contain rich ecosystems (Thorp et al., 2010; Tockner and Stanford, 2002), and are prone to flood risks (Stoffel et al., 2016; Lóczy et al., 2009; Sampson et al., 2015).

Valleys range from narrow, bedrock-confined valleys to wide, alluvial floodplains and glacially carved troughs (Gilbert, 1877; McGee, 1894; Schumm and Ethridge, 1994; Li et al., 2001; Brook et al., 2005). In some cases, valleys can be much wider than the channel they host (Lavé and Avouac, 2001; Farr and Chadwick, 1996) and exhibit various morphologies across climatic, tectonic, and lithological settings. This diversity of shapes results from the range of contexts and processes shaping them.

The width of valleys is one of their major morphologic characteristics. It mostly results from the competition between vertical incision, lateral erosion, and sediment supply (Gilbert, 1877; Bufe et al., 2016; Tofelde et al., 2022; Maddy et al., 2001; Clubb

https://doi.org/10.5194/egusphere-2026-3145
Preprint. Discussion started: 15 June 2026

et al., 2023). As such, valley width is an adjustment variable in landscape dynamics that should be taken into account when studying landscape response to tectonic and climatic changes in terms of topographic evolution (Hancock and Anderson, 2002; Langston and Tucker, 2018), formation of strath terrace, (Lavé and Avouac, 2000), triggering of landslides (Baynes et al., 2022) and sediment storage and release (Schanz and Montgomery, 2016; Finnegan and Dietrich, 2011; Rockwell et al., 1984; Bradley and Tucker, 2013).

Valleys are susceptible to widening through two end-member mechanisms: the lateral erosion of valley walls (Hancock and Anderson, 2002; Langston and Tucker, 2018; Turowski et al., 2024) or the accumulation of sediments within valleys (Clubb et al., 2023). Lateral erosion can happen when the river comes into contact with the valley wall, either because the channel is as wide as the valley, during lateral channel migration across the existing valley floor (Hancock and Anderson, 2002; Brocard and der Beek, 2006; Malatesta et al., 2017), or during flood events (Gupta et al., 2007; Davidson et al., 2024). Valley widening by sediment infilling can occur during periods when rivers are in a depositional regime (i.e. when upstream sediment supply is greater than the channel's capacity to transport this sediment) or through hillslope processes (Tofelde et al., 2022; Malatesta et al., 2017; May et al., 2013; Yanites et al., 2018; Beeson et al., 2018; Lancaster, 2008). In both cases, widening is in competition with channel incision (Gilbert, 1877) which reacts to changes in the base level of rivers as well as to flood events (Whipple and Tucker, 1999; Whipple et al., 2000; Davy and Lague, 2009).

The first control on valley width has been shown to be drainage area (Constantine et al., 2014; Dunne et al., 2010; Tomkin et al., 2003; Zavala et al., 2021; Snyder et al., 2003; Brocard and der Beek, 2006; May et al., 2013), which reflects the impact of discharge on valley width. The mean scaling exponent was shown to be consistent by mechanisms of widening through river lateral migration and lateral erosion (Langston and Tucker, 2018; Turowski et al., 2024). However, the wide range of scalings found by different studies (Beeson et al., 2018; Brocard and der Beek, 2006; Clubb et al., 2022; Harel et al., 2022; May et al., 2013; Schanz and Montgomery, 2016; Snyder et al., 2003; Tomkin et al., 2003) does not excludes other mechanisms and calls for an extensive study of the width/area scaling.

Studies such as Schanz and Montgomery (2016); Brocard and der Beek (2006) have observed an impact of lithology on valley width. Wider valleys tend to form in weaker lithologies, and weaker lithology can also favour mecanisms of erosion through undercutting and slumping of the valley walls.

The third main control on valley width is incision rate (Brocard and der Beek, 2006; Clubb et al., 2023), with lower incision rates correlating with the formation of valley flats (Hancock and Anderson, 2002) and with the deposition of alluvial fills (Clubb et al., 2023).

Other controls include sediment supply by the river and neighbouring slopes covering the valley borders (Tofelde et al., 2022), incision inhibition and enhancing of channel mobility (Turowski et al., 2007; Beer et al., 2017; Baynes et al., 2020), landsliding (May et al., 2013).

While the longitudinal profile of valleys throughout fluvial landscapes has been extensively studied (Horton, 1945; Whipple, 2004; Lague, 2014), the understanding of valley morphology and lateral erosion remains limited (Hancock and Anderson, 2002; May et al., 2013). Indeed, the systematic mapping and quantitative characterization of valley morphology at regional to continental scales remains a challenge (Clubb et al., 2022). Field-based measurements and manual mapping (Brocard and der

https://doi.org/10.5194/egusphere-2026-3145
Preprint. Discussion started: 15 June 2026

Beek, 2006; Lancaster, 2008) are time-consuming and mostly provide discontinuous measurements. Recent advances in digital elevation model (DEM) analysis have enabled continuous measurements of valley floor width along river networks (Clubb et al., 2022, 2023), providing new opportunities to investigate spatial patterns in valley geometry. For systematic mapping purposes, valleys can be defined 1) from a geometrical perspective, as low-slope areas surrounding channels and bounded by steeper and higher valley walls; or 2) from a hydraulic perspective, as areas hydraulically connected to channels and therefore susceptible to flooding during intense rainfall events.

Existing methods for extracting valleys from DEMs primarily rely on a geometrical definition of valleys, using thresholds on slope and elevation (Williams et al., 2000; Clubb et al., 2017; Daxberger et al., 2014; Stout and Belmont, 2014; Degiorgis et al., 2012), or slope breaks at the edges of valleys (Zhao et al., 2019). Extracting valleys based on their hydraulic definition is less common for geomorphic analysis since it requires flood modeling (Noman et al., 2003; Brunner, 2016), which is costly in terms of computing time. In turn, its use is mostly restricted to engineering studies or flood hazard assessment.

The primary goal of this study is to evaluate the benefits and limitations of two different automatic algorithms, based on a geometrical or hydraulic definition of valleys, to map valley extent and quantify valley width. The first is a geometrical method adapted from Clubb et al. (2017), and the second is a new pseudo-hydraulic method that we have developed. This latter method estimates flood-prone valley extent based on a simplified water-filling simulation and a given precipitation depth. This algorithm differs from previous models used to delineate valleys because it does not model the actual flow dynamics but instead computes a synthetic water surface using a water distribution algorithm. We evaluate the accuracy of these methods by comparing them to the distribution of alluvial deposits in four regions spanning contrasting geomorphic settings, in the Western Alps, Pyrenees, Scotland and Taiwan.

The second goal of the study is to study the controls on valley width. After comparing both method we compute width throughout the valley networks of theses four regions and test how drainage area and lithology control valley width.

2 Methods

2.1 Valley detection

The two methods that are compared in this study both require the initial computation of a channel network. We process the digital elevation data using TopoToolbox 3 (Schwanghart and Scherler, 2014; Kearney et al., 2025). We compute drainage area A using a D8 flow routing algorithm, and extract channels using a user-defined drainage area threshold of 5 km^2. This relatively high drainage area ensures that the entire drainage network we extract is composed of well-formed valleys, since channels are mostly initiated around 0.01 km^2 (Montgomery and Dietrich, 1992; Passalacqua et al., 2010; Clubb et al., 2014).

2.1.1 Geometrical approach

The geometrical approach follows a method adapted from Clubb et al. (2017), where valleys are extracted based on two thresholds : one for slope, S_c and one for elevation above channel, H_c. We compute the slope gradient for each DEM pixel

https://doi.org/10.5194/egusphere-2026-3145
Preprint. Discussion started: 15 June 2026

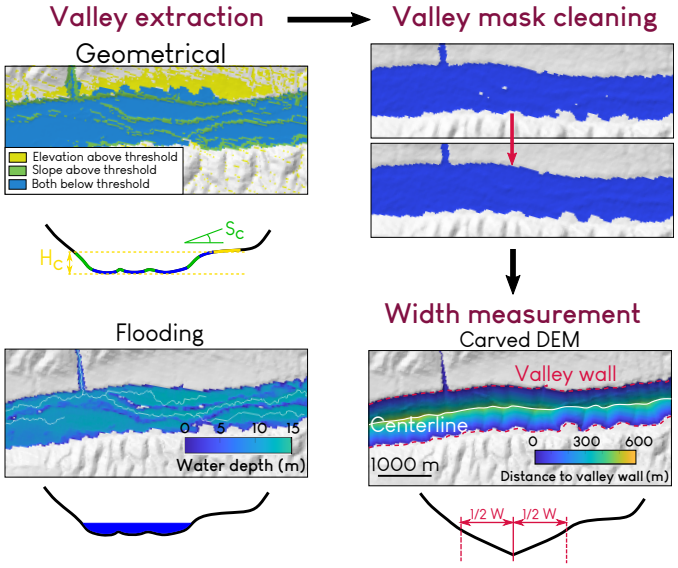

Figure 1. Map view and cross section sketches of valley extraction and width computation for the two methods. The red dotted lines represent the borders of the valley mask after cleaning. The mask cleaning, carving and width computation is shown for the mask obtained with the flooding method, but the process is the same for both methods.

as the steepest downward gradient within the 8 neighbouring pixels. As for elevation above the nearest channel, we use the HAND (Height Above the Nearest Drainage) model (Nobre et al., 2011): for each pixel, we find the nearest stream pixel using a D8 routing algorithm, and we calculate the elevation drop from the initial pixel. The valley mask is then defined as having both a slope lower than S_c and and elevation above the channel lower than H_c (see Figure 1, upper left panel). The valley mask may present holes in places because steep slopes can be found locally even at the bottom of a valley (e.g., river banks or noise, Schwanghart and Scherler (2017)). Following Clubb et al. (2017), we perform two cleaning operations to fill these holes: (1) a morphological image filling followed by closing, which removes small holes and smooths the valley shape, and (2) a filling of isolated holes enclosed by valley pixels.

2.1.2 Flooding approach

This new pseudo-hydraulic approach defines valleys as the area around streams susceptible to flooding. Rather than solving for flow inundation patterns using 2D shallow water equations (Gailleton et al., 2024; Pons et al., 2026), which is computationally expensive, our method distributes a volume of water, dependent on the drainage area A around each stream pixel, to yield a flat water surface. We compute this volume of water V to be distributed around each stream pixel using A weighted by a precipitation height P. This precipitation height is not necessarily representative of actual effective precipitation, but rather represents a precipitation height required to flood the entire valley floor. A window over which water is spread has to be defined. The width w of rivers and valley increases downstream with approximately the square root of drainage area (Leopold

https://doi.org/10.5194/egusphere-2026-3145
Preprint. Discussion started: 15 June 2026

and Maddock, 1953): a circular window of radius $R = c\sqrt{A}$ is therefore chosen, where c is a prescribed prefactor. If assuming a constant but not defined mean alongstream flow velocity v, spatial continuity of water discharge $Q = wdv$, and that discharge is proportional to A, the ratio of V/R leads to a theoretical equivalent valley - or river during flood - depth :

$$d \propto \frac{P}{c}\sqrt{A} \tag{1}$$

This theoretical framework underlying this pseudo-hydraulic approach is therefore close to empirical scaling relationships with drainage area of valley or river width $w \propto A^{0.5}$, and water depth $d \propto A^{0.4}$, but neglects the slight dependence of water velocity with drainage area $v \propto A^{0.1}$ that is generally observed (e.g., Leopold and Maddock (1953)). In particular, this new approach distributes water so that water depth scales with $\sqrt{A}$, which is critical to avoid overflowing over the valley borders. Yet, we note that this approach does not prescribe the resulting valley width or its scaling with A, which we will later demonstrate is an emerging feature, but rather bounds its maximum value to $2R$ or $2c\sqrt{A}$.

Practically, the water filling algorithm sorts pixels within the window by elevation and calculates the theoretical volume of water necessary to reach the height of each pixel in the sorted list, computed as :

$$V(i) = \sum_{n=1}^{i} ndx^2 dh(n) \tag{2}$$

where i is the number of the considered pixel, dx is the pixel size, and $dh(n)$ is the elevation difference between the pixels being filled and the following pixels in order of elevation. This allows us to determine which pixels are going to be filled, as a function of the imposed volume V and the height of water at each of them. The remaining volume is evenly distributed on the water surface. We then get a local map of water depth d within the window (see Figure 1, lower left panel). This operation is repeated for every pixel in the stream network. Pixels which are visited multiple times record only the maximum depth that was distributed to that pixel. The valley mask is then simply obtained by extracting pixels where the water depth is greater than zero. We apply the same post-processing as described in the previous section (morphological closing and filling isolated zeros) to get a clean valley mask.

2.2 Valley width measurement

Once a valley mask is obtained, the next step towards computing valley width W consists in extracting the centerline of the valley as in Clubb et al. (2022). To do so, we first identify the pixels located on the valley mask borders. We then compute the Euclidean distance d_w between each valley pixel to the nearest valley mask border. We then compute a carved DEM z_{carved} which consists of the actual DEM elevation z minus a term which is a function of this distance:

$$z_{carved} = z - \alpha d_w, \tag{3}$$

where α is a user-defined parameter that we set to 0.5. A new flow direction map can then be recomputed on this carved DEM and a new stream network flowing at the center of valleys is obtained (see Figure 1).

Several approaches can then be defined to measure the width of the valley mask from the valley centerline. The simplest approach is to compute the nearest distance from the valley centerline to the valley borders, as it is readily obtained by taking

https://doi.org/10.5194/egusphere-2026-3145
Preprint. Discussion started: 15 June 2026

d_w at the valley centerline. Valley width W is then simply $2d_w$. This approach is deemed simpler and quicker than to compute W in the orthogonal direction to the valley centerline (Clubb et al., 2022), as it does not require to compute stream orientation or to find the intersect between the orthogonal line and the valley border. Once defined along the valley centerline, W can be clipped to the initial network, for instance through a nearest neighbour search.

2.3 Algorithm calibration from alluvial data

We test the valley extraction methods using 30 m resolution DEMs from NASA SRTM data (Farr et al., 2007) in four mountainous regions: the Western Alps, the Pyrenees, the Scottish Highlands and the Central Range in Taiwan. These regions are located in landscapes displaying different geomorphic contexts, including steep and active mountain ranges, lower-relief foothills, and glacially-influenced landscapes. This selection ensures robust performance assessment for the two valley extraction methods across different geomorphic settings.

To assess the accuracy of valley extraction, an independent dataset representative of valley extent is required. Manual delineation of valley floors from hillshade visualizations is feasible; however, its reliability decreases as valley morphology departs from a well-defined, flat valley floor. Consequently, we chose to compare valley outlines with geological maps of alluvial deposits (see Figure 2). Alluvial deposits serve as proxies for the spatial extent of fluvial activity over geomorphic timescales, under the assumption that the rivers were predominantly in a depositional regime. We retrieved alluvial deposits from 1/50000 digital regional geological maps produced by the French Bureau de Ressources Geologiques et Minières (BD-charm), the British Geological Survey and Taiwan Central Geological Survey (Landslide Cloud).

Using alluvial data to map valleys relies on a couple of assumptions which may be a source of error in the delimitation of valleys. First, it implies that alluvial deposits cover the entirety of the valley, which might not always be the case, in particular along upstream valleys which can be dominated by fluvial or glacial bedrock incision in active mountain ranges or in cold climates, respectively. We partly limit the issue of bedrock valleys by only extracting valleys above a relatively high drainage area of 5 km^2, therefore maximizing the chance for the extracted rivers to be in a transport-limited regime. Secondly, it implies that all alluvial deposits are currently inside valleys. Ancient alluvial deposits can be uplifted or incised and therefore form alluvial terraces that are not part of the modern valley floor. Based on the comparison of topography and alluvial deposits, we chose to include sediments dated from the Last Glacial Maximum to Holocene times in the analysis.

2.3.1 Data and study sites

The first region is located in the Western Alps in Southeast France (see Figure A1). The region extends over an area of 16,600 km^2 and includes the catchments of the Durance and Buëch rivers. Most of the north and eastern part of the region are located above the altitude of the ice extent during the lst glacial maximum. The elevation ranges between 250 m and 3700 m, and mean slope is 0.34. This is a mountainous catchment covering the subalpine and external crystalline massif (Schmid et al., 2004), with a low tectonic activity (Champagnac et al., 2007). This area is characterized by high slopes and the dominance of mass-wasting processes in headwater areas (Cossart et al., 2008). In the south of the region, tertiary molassic catchments form plateaux of weakly consolidated sediments incised by fluvial valleys and debris-flows (Godard et al., 2020).

https://doi.org/10.5194/egusphere-2026-3145
Preprint. Discussion started: 15 June 2026

The second region extends from the Spanish border in in the axial and northern zones of the Pyrenean range to the Adour and Gave de Pau basins in the Pyrenean foreland basin to the north. The region covers an area of 10,500 km^2. The elevation in the region varies from 70 m to 3260 m and the mean slope is 0.5429. The mountainous part of the region is underlain by Paleozoic and Mesozoic sediments, as well as granitic massifs (Roest and Srivastava, 1991; Rosenbaum et al., 2002; Vissers and Meijer, 2012; Zwart, 1979; Capote et al., 2002). The foothill domain is composed of Cenozoic fluvial sediments (Ford et al., 2016; Rougier et al., 2016). They are mainly weakly or not consolidated and organized in terrace formations cut by channels. This part of the region is mainly low-relief and low gradient, whereas the southern upstream part is steeper and affected by mass wasting processes.

The third region is located in the northwest Scottish Highlands north of the Great Glen Fault. Its total area is 3,858 km^2. The altitude ranges between 0 m and 1160 m and mean slope is 0.12. It has been primarily shaped by glacial erosion of the underlying metamorphic rocks during the Quaternary period (Clark et al., 2022; Bickerdike et al., 2018). This resulted in glacial cirques and glacially eroded valleys (Clark et al., 2022). The Holocene period was characterized by uplift due to glacio-isostatic adjustment and enhanced paraglacial landscape adjustment following deglaciation (Ballantyne, 2008), leading to mass movements on hillslopes, and incision, glacial sediment reworking, and aggradation in valleys.

The fourth region is located on the Taiwan island. Its total area is 42,371 km^2. The elevation ranges between sea level and 3900 m and the mean slope is 0.55. The region is tectonically active due to its location at the boundary of the Eurasian and Philippine Sea tectonic plates (Seno, 1977; Suppe, 1984), with high uplift rates around 5 mm/yr (Peng et al., 1977). Intense seismic (Yi-Ben, 1986) and monsoon activity (Chen and Chen, 2003) result in intense geomorphic activity with rainfall-induced landslides and debris flows (Lin and Jeng, 2000; Cheng et al., 2005) as well as fluvial erosion (Willett et al., 2003). In terms of geology, the mountain belt is mainly composed of volcanic rocks and metamorphosed sediments.

2.3.2 Alluvial deposits

Alluvial deposits are widespread in every region (see Figure 2), with some disparities. In the Western Alps and Pyrenees, while downstream valleys and valleys located in the foothill areas are covered with alluvium, headwater valleys in mountainous areas have limited alluvial cover. This trend is even more pronounced in Taiwan, where alluvial deposits are limited and completely absent in upstream reaches. In the Northwest Scottish Highlands region, the alluvial cover is discontinuous in some downstream valleys as well.

2.3.3 Calibration from F1 score

We then seek to find the parameters that yield the best consistency between valley masks, obtained with the flooding or geometrical method, and the alluvial masks. We rely on the F1-score, which measures the predictive performance of the two methods in their parameter space. We first identify the True Positive (TP), False Positive (FP), and False Negative (FN) valley pixels and then compute the F1-score using the following formula:

$$F1 = \frac{2TP}{2TP + FP + FN} \tag{4}$$

https://doi.org/10.5194/egusphere-2026-3145
Preprint. Discussion started: 15 June 2026

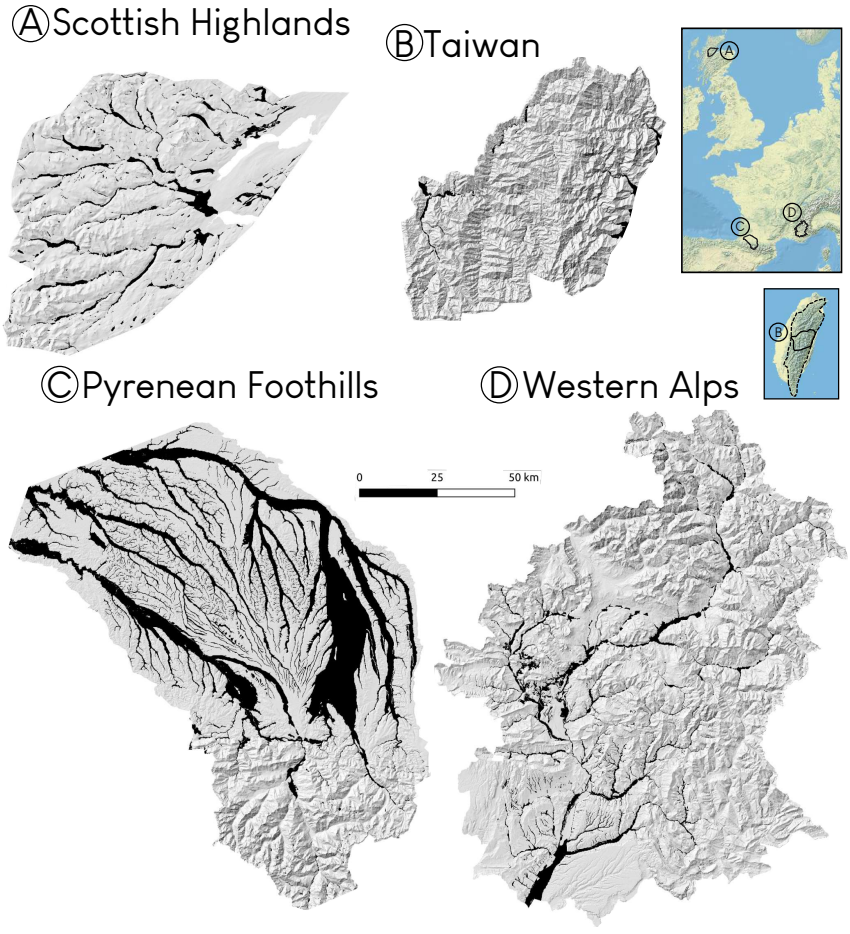

Figure 2. Hillshade maps of the four study regions. The black areas represent the extent of alluvial cover as mapped by regional geology surveys.

https://doi.org/10.5194/egusphere-2026-3145
Preprint. Discussion started: 15 June 2026

For the geometrical method, we vary S_c from 0.03 to 0.2 and H_c from 1 to 43 m. The maximum values were chosen deliberately higher than what could be reasonably expected for valley bottoms to capture the optimal values. For the flooding method, precipitation height P ranges from 1 to 17 mm and the radius prefactor c from 0.04 to 0.14.

2.4 Width-area scaling relationship and wideness index

As discharge and drainage area are expected to be the principal controls over valley width (Constantine et al., 2014; Dunne et al., 2010; Tomkin et al., 2003; Zavala et al., 2021), we focus part of our study on quantifying the scaling relationship between W and A. After computing W and A along the drainage network, we bin the data following A using logarithmically distributed bins. We then perform a least squares linear regression on the log-transformed data in order to retrieve a power-law scaling relationship between W and A :

$$W = K_w A^b \tag{5}$$

Where K_w is a constant and b is the width scaling exponent.

Once the scaling exponent is obtained at the scale of each region, we can define a valley wideness index (Dahlquist and West, 2022) similar to the channel steepness index (Kirby and Whipple, 2001), by normalizing width with respect to drainage area. Given 5, the valley wideness index K_{wn} is :

$$K_{wn} = \frac{W}{A^b} \tag{6}$$

The wideness index allows us to investigate local width variations controlled by factors other than solely drainage area.

3 Results

3.1 Method calibration

Overall, the maximum F1-scores exceed 0.55 for all regions and methods, except in Taiwan (Figure 3). The highest values (~ 0.7) occur in the Alps and Pyrenean Foothill regions, which are predominantly alluvial catchments.

In the Alps, the best-fitting parameters are $H_c = 12$ and $S_c = 0.16$ for the geometrical method and $P = 0.003$ and $c = 0.08$ for the flooding method. The whole range of tested parameter results in f-1 scores above 0.6 for the flooding method, showing a low sensitivity to parametrization. Using the best-fitting parameters, the valley networks obtained with both methods are similar to the extent of alluvial cover (see figure 4) except for two areas: large false negative areas appear in the west and false positive areas can be found in the southern part of the main trunk. These differences will be analyzed in the following section.

In the Pyrenean Foothill region, the maximum F1-score for the flooding method may lie outside the tested parameter range. However, since values remain above 0.7 across the entire parameter space, parametrization appears to have little influence on the flooding method in this catchment. As for the geometrical method, best parameters are $H_c = 7$ and $S_c = 0.16$.

https://doi.org/10.5194/egusphere-2026-3145
Preprint. Discussion started: 15 June 2026

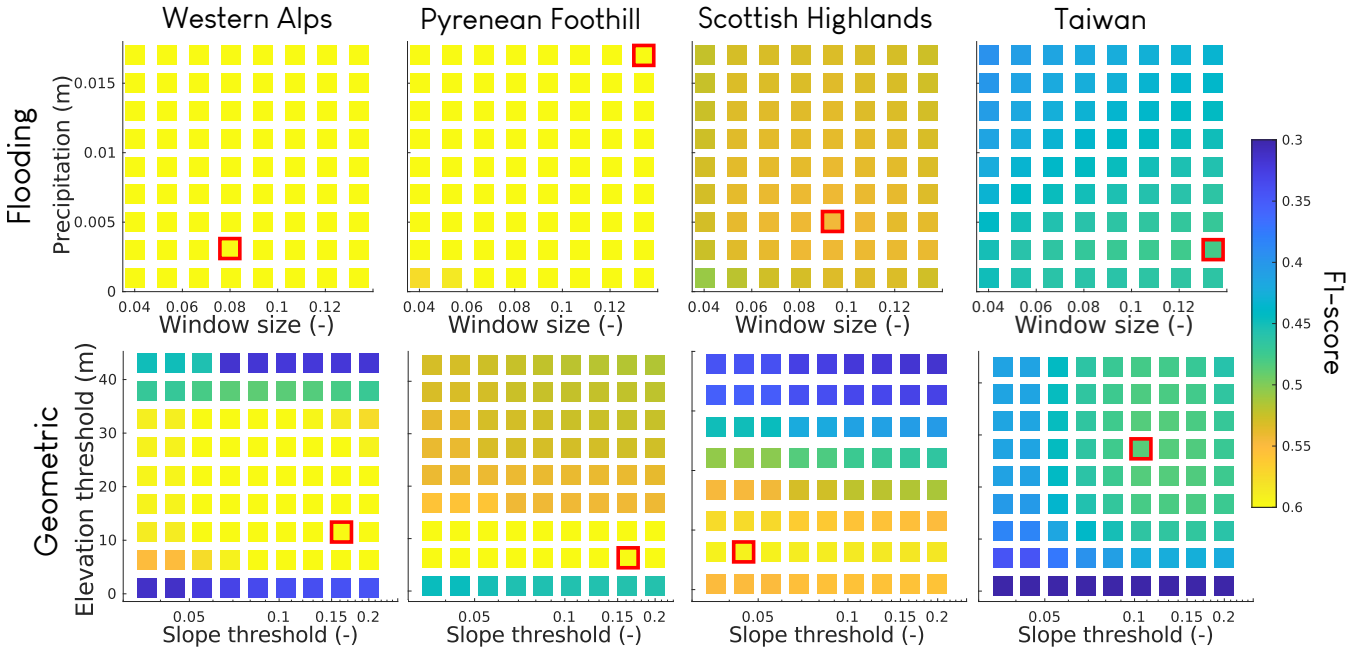

Figure 3. Distribution of F1-score for the flooding and geometrical valley extraction methods in their parameter spaces. Each square represents one experiment, color coded with the corresponding F1-score when compared to the alluvial data. The experiment that yields the highest F1-score for each method and region is highlighted in red.

F1-scores are slightly lower in the Scottish Highlands, with 0.55 and 0.60 for the flooding and geometric methods, respectively, but show the same pattern of sensitivity to the parameters, only with a lower best slope threshold $S_c = 0.045$ consistent with lower slopes throughout the region. We postulate that the lower f-1 score in this area is due to the widespread occurrence of unalluviated low-order valleys (see supplementary Figure A2).

Taiwan stands out as the only region with markedly lower F1-scores. They reach 0.48 for the flooding method and 0.50 for the geometric method. This likely reflects the near absence of mapped alluvial deposits across much of the Central Range (see Figure 2), either due to incomplete mapping or more likely because many valleys are primarily bedrock-dominated. As a result, false positives dominate the metric, making the F1-score difficult to interpret. Furthermore, valleys might be narrower than the pixel size in most of the valley network, which is one limit of using 30 m DEM for valley extraction.

Overall, optimal parameters are broadly consistent across regions. For the flooding method, the optimal P ranges from 3 to 5 mm and c from 0.08 to 0.13. For the geometric method, the optimal H_c varies between 6 and 13 m, except in Taiwan where it is higher at 25 m. The optimal S_c ranges from 0.05 to 0.16, although the F1-score shows little sensitivity to S_c except in Taiwan.

The main difference between the geometrical and flooding methods is their different sensitivities to parametrization. The flooding method is comparatively robust, with F1-scores varying little across the tested parameter domain. In contrast, the geometric method is sensitive to H_c, with F1-scores ranging from about 0.3 to 0.7 when varying it. S_c has a weaker influence

https://doi.org/10.5194/egusphere-2026-3145
Preprint. Discussion started: 15 June 2026

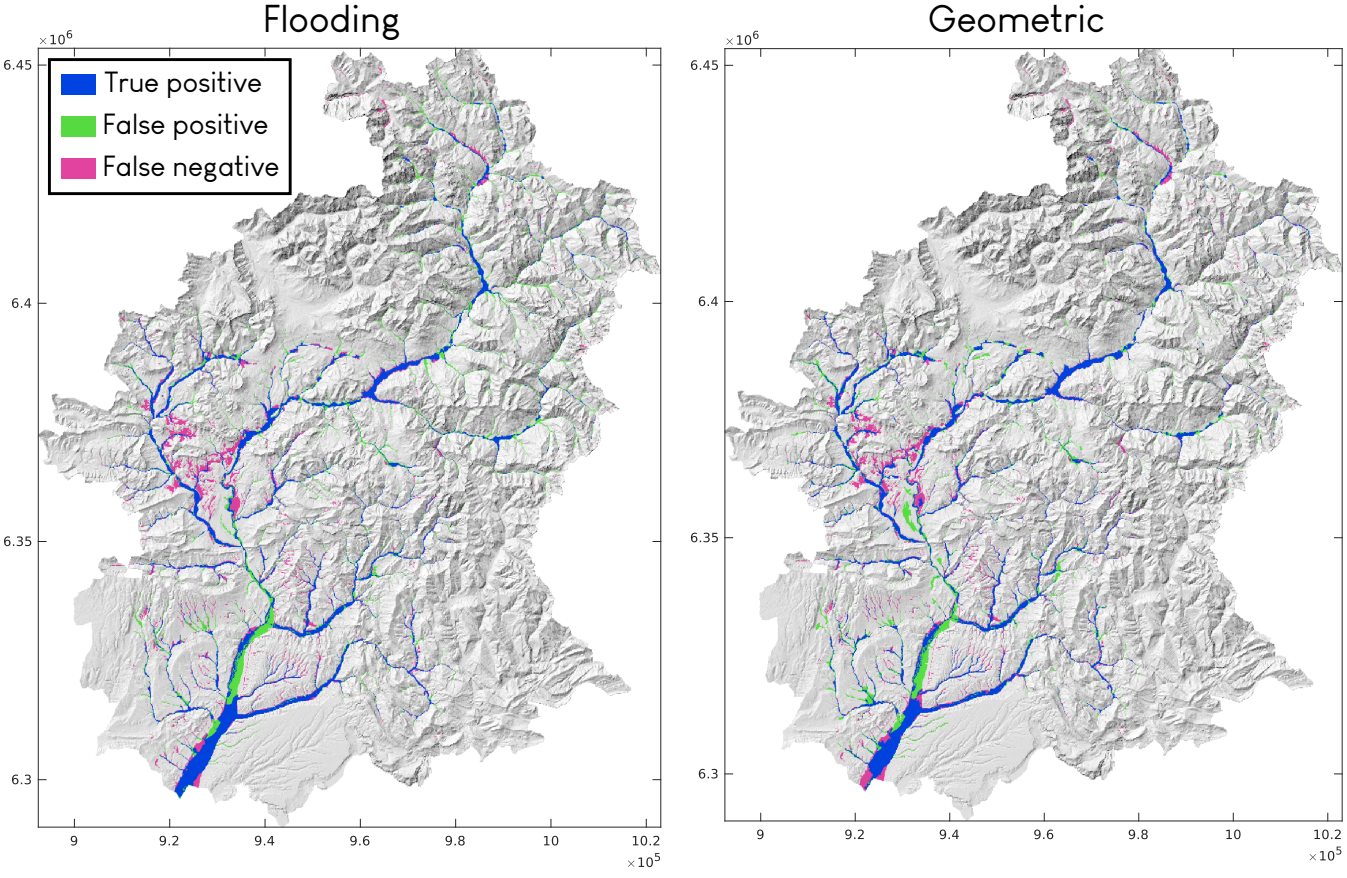

Figure 4. Map of true positive (blue), false negative (pink) and false positive (green) pixels for both methods in the Western Alps region.

provided it remains above 0.03. In general, values of H_c between 7 and 15 m and S_c between 0.05 and 0.2 yield higher F1-scores. In the remainder of this paper, valley extraction results are analyzed using the parameter set that produces the highest F1-score for both methods (Figure 5).

3.2 Valley characteristics

Upon visual inspection, both methods are performing well at identifying valleys (Figure 5). However, some systematic differences appear, especially in low drainage area valleys. In the mountainous domains of the Pyrenees, Western Alps and Taiwan, upstream valleys are slightly wider when extracted with the flooding method. In these cases, the steep valley walls limit the extent of the valley extracted using the geometrical method, while the water filling algorithm of the flooding method can extract wider valleys depending on the amount of available water. The opposite goes for the Valensole plateau, South of the Western Alps selected region, and for the foothill area in the Pyrenees. In these low-relief areas, the geometric method identifies flat areas that are wider than the valleys as deduced from the flooding method. In the Scottish Highlands region, the valley network

https://doi.org/10.5194/egusphere-2026-3145
Preprint. Discussion started: 15 June 2026

is dominated by widened valleys occupied by lakes (dark gray areas on Figure 5) alternating with narrow incised valleys. The eastern part of the region is a low-relief area surrounding the coast without well distinguished valleys. The same differences between the two methods appear in upstream reaches.

3.3 Valley width-area relationship

The width-area relationships for all catchments and the two methods, as well as for the alluvial deposits, are shown in Figure 6. They all exhibit a strong correlation between W and A, except for Taiwan. In Taiwan, most valleys seem to be narrower than the DEM resolution, resulting in single pixel-valleys whose widths are constrained by the 30 m DEM resolution. In this study, we excluded widths below or equal to 60 m from the regression because we consider that they do not reflect the actual width of the valley.

Overall, the scaling exponents b obtained with the flooding method and the geometrical method are similar: they are 0.48 and 0.45 in the Western Alps, 0.44 and 0.36 in the Pyrenean foothills, and 0.24 and 0.39 in the Scottish Highlands, respectively. This scaling is consistent with previous studies of valley widths (Brocard and der Beek, 2006; Clubb et al., 2022; Langston and Temme, 2019; May et al., 2013; Schanz and Montgomery, 2016; Turowski et al., 2024) that mainly found width-area scaling exponents around 0.3-0.4.

However, some differences emerge between the different methods. First, because alluvial deposits are largely absent upstream, the alluvial mapping method results in narrow upstream valleys, leading to higher scaling exponents. Second, the correlation between width and drainage area (i.e. the R^2) is consistently stronger in the case of the flooding method. This illustrates how the conceptual distinction between morphological and hydraulic definitions of valleys affects valley width–area analysis. Since the flooding method explicitly distributes water volumes as a function of A, W can be partially constrained by drainage area, especially in the more confined upstream valleys where the quantity of water which is distributed affects the water height and therefore the width of the resulting valley. This results in higher R^2 values when computing the slope-area relationship.

3.4 Valley wideness index

Local variations of wideness index, K_{wn}, seem to correlate with geological features in the Western Alps, Pyrenean Foothills and Scottish Highlands regions (Figure 7). In the Pyrenean foothill region, K_{wn} shows a noticeable negative anomaly in the southern mountainous part of the region (see Figure 7(a)), which was not detectable in the width-area scaling relationship (Figure 6). The boundary of this negative K_{wn} anomaly coincides with the geological contact between Mesozoic sedimentary rocks in the mountain range and Tertiary poorly consolidated rocks in the foothills (see figure A1). In this case, this limit also coincides with the Northern Pyrenean Frontal Thrust (NPFT), which is a tectonic boundary between the uplifted and deformed range and the foothills (Lacan and Ortuño Candela, 2012; Curry and van der Beek, 2025). Even at a finer kilometric scale, the impact of lithology on K_{wn} is visible in the East of the studied region in the Pyrenees foothills (Figure 7(b)). The valley network successively runs through the units: Cretaceous flyschs, Eocene-age limestones, and Eocene-Miocene conglomerates

https://doi.org/10.5194/egusphere-2026-3145
Preprint. Discussion started: 15 June 2026

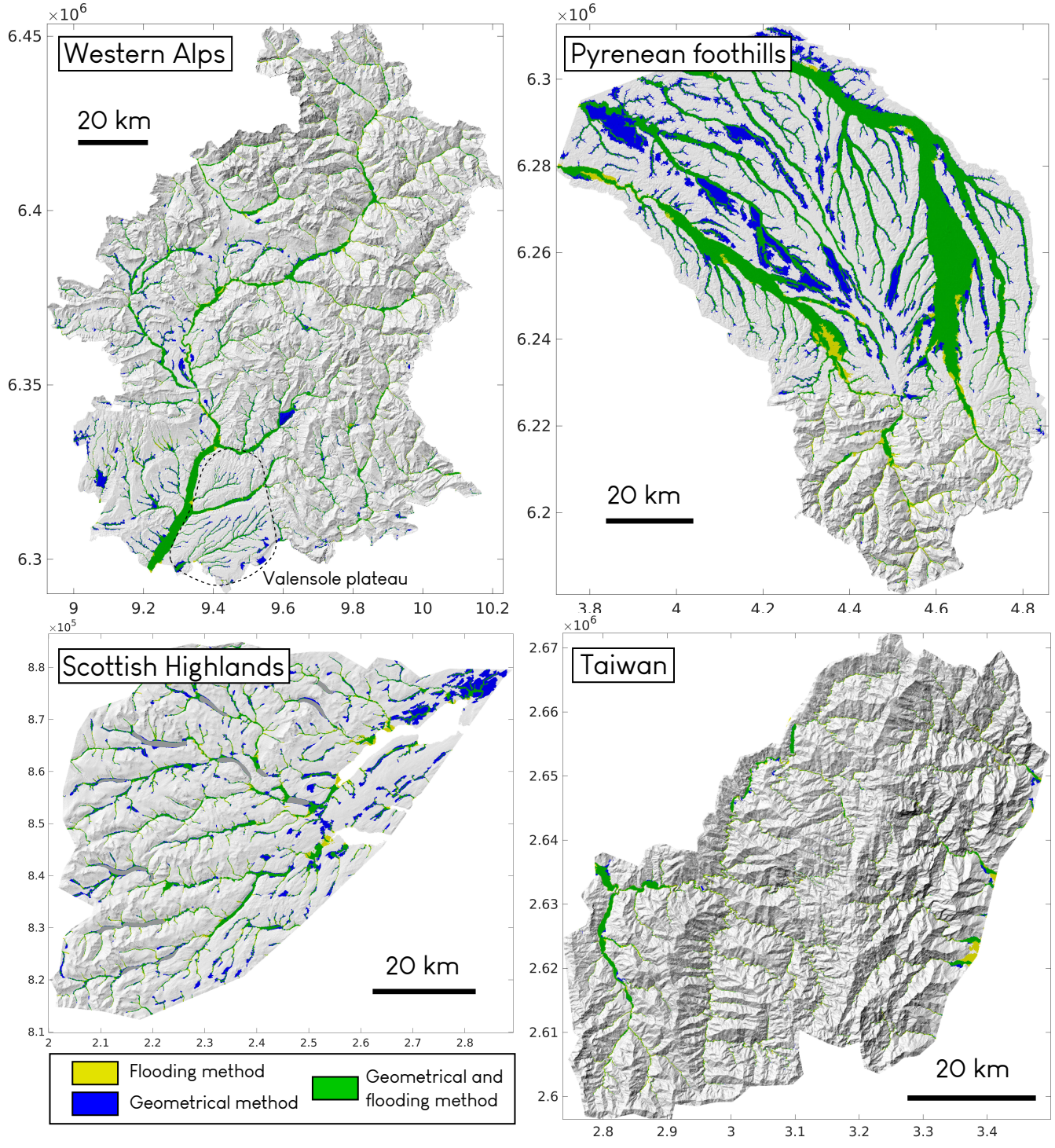

Figure 5. Map of the results of the valley extractions using both methods calibrated from the best F1-score experiment. Blue areas show the valleys extracted by the geometrical method; yellow areas show the valleys extracted by the flooding method. Areas classified as valleys by both methods are coloured in green. Grey areas in the Scottish Highlands region represent lakes.

https://doi.org/10.5194/egusphere-2026-3145
Preprint. Discussion started: 15 June 2026

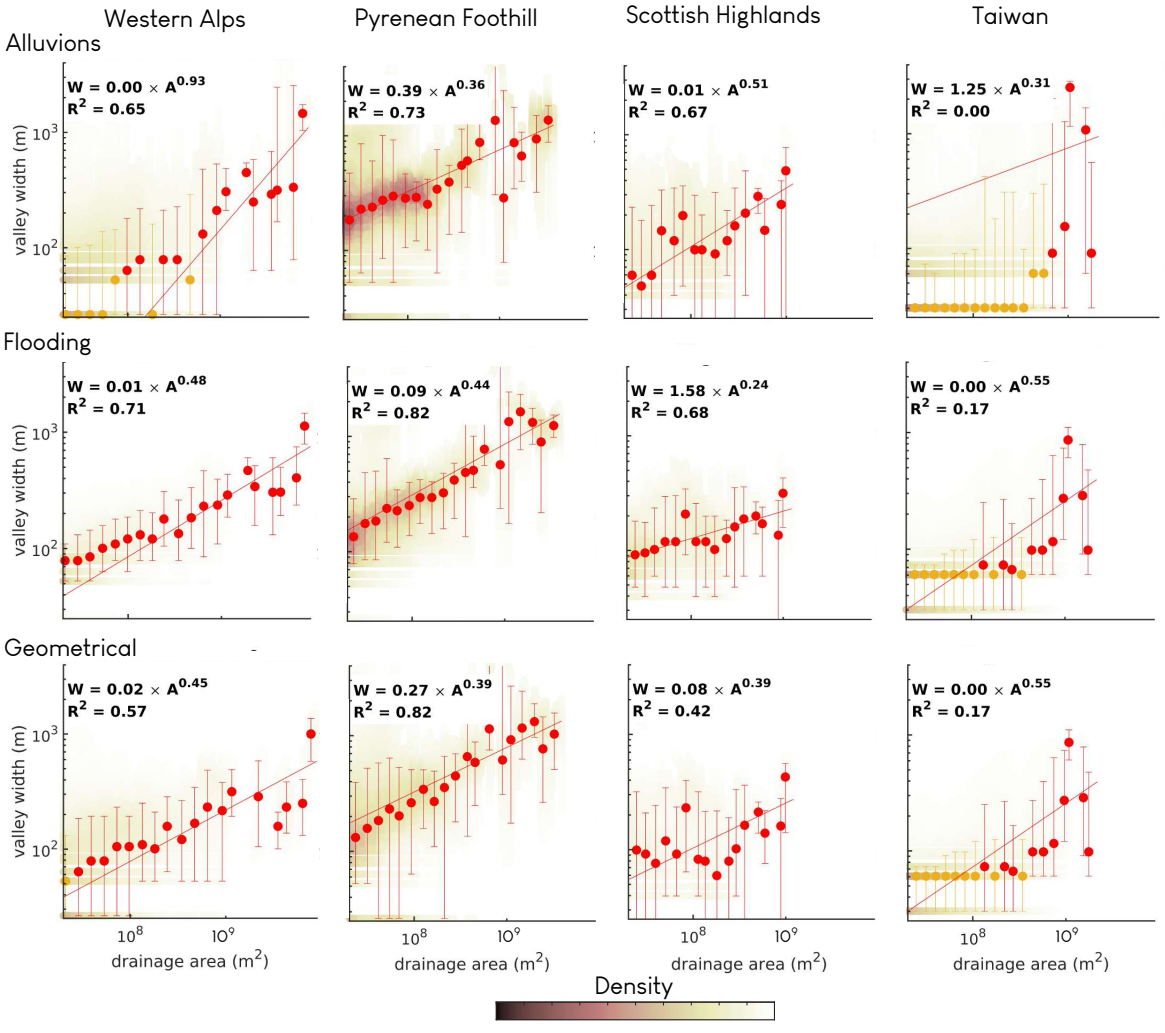

Figure 6. Width-area relationships and power-law fits for geometrical, flooding and alluvial valley masks. Distributions of data density is represented with the background colormap. The red dots represent the bins used for the power law fit, while the yellow ones are excluded from the analysis because they are associated to width below or equal than than two pixels.

https://doi.org/10.5194/egusphere-2026-3145
Preprint. Discussion started: 15 June 2026

and alluvium. The contact between geological units is imprinted at a fine scale in the pattern of valley width and wideness index.

When examining the wideness index in first-order formerly glaciated valleys in the Scottish Highlands (see Figure 7(c)), where bedrock lithology is near uniform, one pattern appears in several valley heads: the initiation of valleys occurs in glacial cirques characterized by a positive wideness index anomaly. Valleys then narrow in the downstream direction in most cases before joining the main and higher order stem, which is either a wide valley or lake or a narrow incised channel.

In the Western Alps region, focusing on the trunk of the valley network, a sharp contrast appears between the southern valley, characterized by a weakly positive wideness index, and the northern part, with a negative wideness index (see Figure 7(d)). As shown in Supplementary Figure A1, lithology does not seem to be the main control here. The difference lies in the fact the in the northern part, the river has incised recent Wurm alluvial deposits and narrowed its valley to form strath terraces, while in the southern part, the deposits are not incised, yielding a wide alluvial floodplain.

4 Discussion

4.1 Benefits and limitations of the valley extraction methods

Comparison of the geometrical and flooding valley extraction methods highlights trade-offs between robustness, adaptability, and computational efficiency. Although both methods can be calibrated to achieve relatively similar performances, they differ in their sensitivity to parameter selection, computational cost, and suitability for downstream analyses. Overall, these differences reflect the distinct conceptual definitions of what constitutes a valley underlying both methods.

The flooding method exhibits a low sensitivity to parameter choice, with the F1-score remaining relatively stable across a broad parameter space. This robustness suggests that the method is less dependent on parametrization. Indeed, assuming that valleys are bounded by hillslopes, the flooding pattern is unlikely to change significantly when increasing P once the water level has reached the valley walls. Similarly, if the choice of the radius is sufficiently large to prevent bounding the effective valley width, this parameter should have a limited effect on the resulting valley masks and widths. In turn, the flooding method is expected to produce more reliable results when applied across heterogeneous regions where optimal parameters can vary. As an example, the flooding method responds well to the contrast between the mountainous upstream region and the lower-relief foothills in the Pyrenees, while the geometric method struggles to accurately capture valleys in low-lying parts of the landscape. In contrast, the geometrical method is more sensitive to parameter selection, particularly to the elevation-above-channel threshold. While this sensitivity requires careful calibration, it also makes the geometrical method more flexible when extracting specific geomorphological features associated with valleys. Indeed, using higher H_c thresholds enables the identification of terraces within valleys, and potentially the separation of different levels of staircase terraces.

Computational efficiency further distinguishes the two methods. The flooding approach is substantially more computationally intensive due to repeated water-filling operations around each stream pixel, resulting in increased processing time and memory usage. The computing time of the flooding method varies as a power law of the window size parameter d with an exponent of 1.7. On average, for $d = 0.1$, the flooding method is a hundred times slower to retrieve valley masks than the

https://doi.org/10.5194/egusphere-2026-3145
Preprint. Discussion started: 15 June 2026

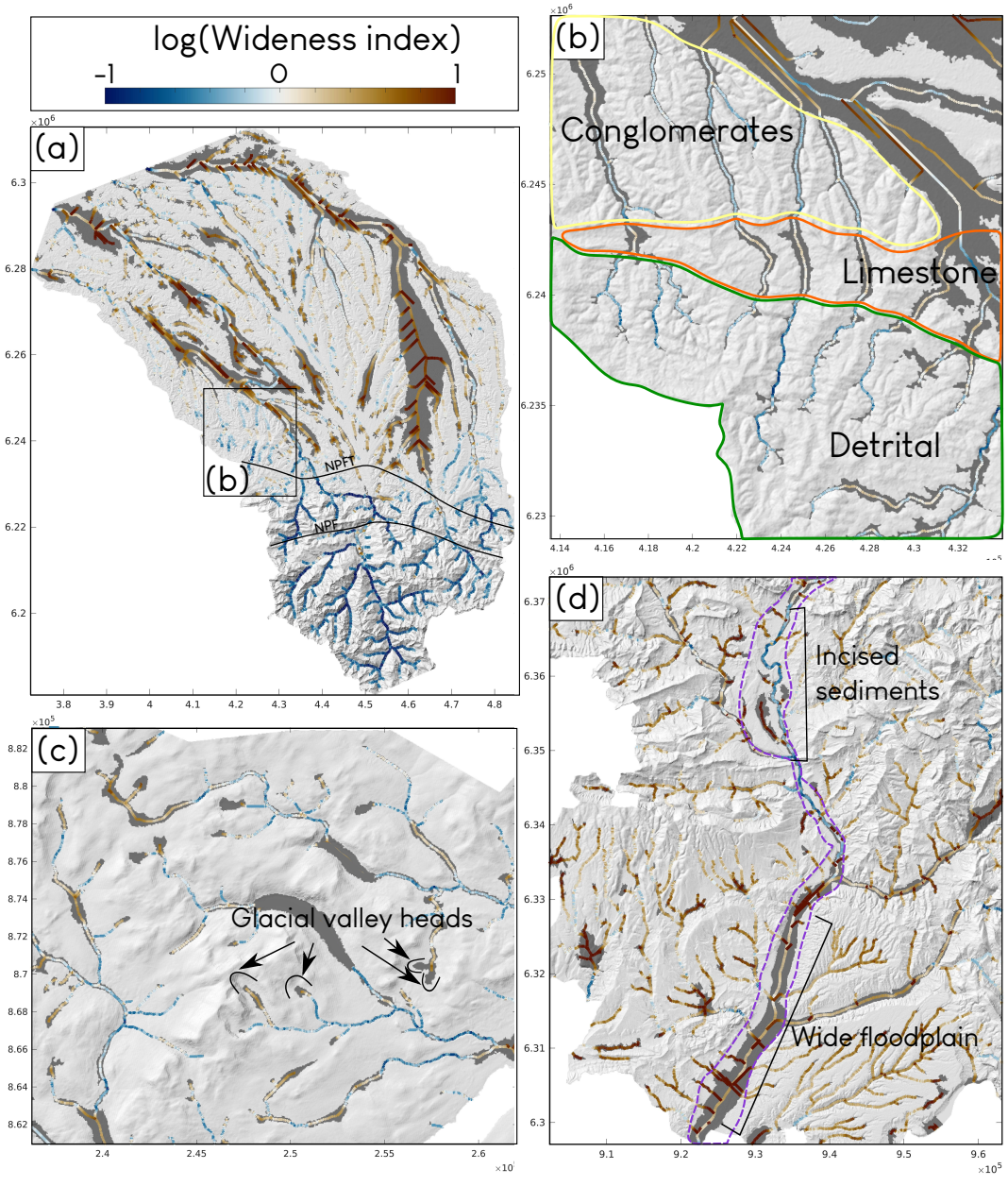

Figure 7. Maps of K_{wn} along the stream network for the valleys extracted with the geometrical method. Gray areas in the hillshade maps show the extent of the mapped valley floor. The drainage network is superimposed and color-coded with the $log(K_{wn})$ computed for each channel pixel.

https://doi.org/10.5194/egusphere-2026-3145
Preprint. Discussion started: 15 June 2026

geometrical method, which relies on local topographic metrics that are only computed once for every pixel. In catchments covering around 10,000 km^2 such as those studied, the computing times is around 0.5 seconds for the geometrical method and 50 seconds for the flooding method.

Overall, the flooding method is best suited for applications requiring robust and conservative estimates of flood-prone valley extent, particularly where parameter calibration is challenging. The geometrical method, while more sensitive to parameter choice, offers greater flexibility and lower computational cost, and is best suited for valley width calculation across large spatial scales or on large DEMs.

4.2 Valley width-drainage area scaling relationships

By providing continuous valley masks and width measurements along river networks, both methods enable thorough characterization of valley geometry at the scale of entire catchments or landscapes.

Previous studies have shown that drainage area and lithology are primary controls on W (Clubb et al., 2022; Beeson et al., 2018; Brocard and der Beek, 2006; Langston and Tucker, 2018; May et al., 2013; Schanz and Montgomery, 2016). Our results in the Western Alps, Pyrenean foothills and Scottish Highlands regions confirm the role of A, with the b exponent varying between 0.2 and 0.6. Turowski et al. (2024) compiled b exponents from several studies, finding variable exponents with an average value of 0.29, and a standard deviation of 0.35. Our results therefore agree with previous findings, including in the glacially-influenced landscape of the Scottish Highlands. This scaling is consistent with physics-based models of valley widening through lateral erosion by migrating fluvial channels (Langston and Tucker, 2018; Turowski et al., 2024). Furthermore, the variability of the b scaling exponent between regions shows that the dependence of valley width on drainage area is also modulated by lithology (Langston and Temme, 2019; Langston and Tucker, 2018; Clubb et al., 2022), tectonics (Clubb et al., 2023), hillslope sediment supply (Tofelde et al., 2022; Groeber and Langston, 2024), and climate.

We found a lower b exponent (0.24) in the Scottish Highlands region when using the flooding method compared to that obtained with the geometrical method (0.39). It seems to be mainly due to the higher dispersion in the data obtained with the geometrical method which results in a less robust scaling, and maybe to the high width found in the downstream part of the network where the landscape is mostly flat. If we focus on the flooding method, the low scaling exponent may be due to the fact that headwater valleys are wider due to glacial modification of valley floors during the Quaternary, as suggested by the high (1.58) prefactor in the power-law regression. This relatively low b exponent is consistent with previous results and with theoretical models of glacial valley formation dominated by abrasion (Bernard et al., 2021). However, it needs to be confirmed through the global and systematic extraction of this scaling in different tectonic and climatic settings. Indeed, most studies of valley width focus mainly on fluvial valleys, and on the mechanisms of widening through fluvial erosion therefore we lack data on glacial valley width.

The use of automatic valley detection methods like the ones presented in this study, which are simple and applicable to any confined valley system, whether they are fluvial, glacial, alluvial, or bedrock valleys, could help clarify the controls on valley width-drainage area scaling and therefore valley widening processes, especially when coupled with methods that assess the fluvial or glacial origin of valleys such as those of Prasicek et al. (2015) or Zimmer and Gabet (2018).

https://doi.org/10.5194/egusphere-2026-3145
Preprint. Discussion started: 15 June 2026

4.3 Geological and tectonic controls on local wideness index anomalies

Computing the scaling of valley width with drainage area also allows the normalization of width through the use of the valley wideness index. It can be used to identify anomalously wide or narrow valley segments compared to their drainage area along river networks. These anomalies may reflect spatial variations in valley width driven by other controls than drainage area, such as lithology (Keen-Zebert et al., 2017; Brocard and der Beek, 2006; Schanz and Montgomery, 2016), structural controls, sediment supply variations and landslides (Yanites et al., 2018; Beeson et al., 2018; Clubb et al., 2023; May et al., 2013), or drainage reorganisation (Harel et al., 2022).

The results we obtain highlight two main controls, namely tectonics and lithology (Figure 7). We plotted the distribution of the logged wideness index as a function of the lithology in the Western Alps and Pyrenean Foothills which are the two regions where lithology varies the most (see Figure 8). This figure suggests some level of control of lithology on width as the hardest rock types, such as the plutonic and metamorphic rocks, exhibit lower K_{wn}, while the less resistant rock types, such as poorly consolidated sediments, coarse detrital rocks or marls, have higher K_{wn}. Rock types such as limestones (e.g., variable composition or bed thickness), sandstones (e.g, variable diagenetic grade) or volcanic rocks (e.g., from weak tuff to strong basalts), which likely encompass a wide range of rock erodibility, do not exhibit distinct trends in valley wideness index.

In the Pyrenees, disentangling the tectonic and lithologic controls is difficult since the NPFT is both a lithologic and tectonic boundary. However, our results suggest that tectonics could have an impact on valley width, as the northern part of the mountain range, between the North Pyrenean Fault (NPF) and the NPFT, which has lower relief, than the southern part but wimilar lithologies, has fewer negative wideness index anomalies. Similar tectonic controls on valley width have been observed across the Himalayan mountain range, suggesting tectonic structures may be a key control on local variations in valley width (Clubb et al., 2023).

4.4 Characterizing valley morphology

Valleys exhibit various morphologies, from wide, U-shaped glacial valleys to confined V-shaped valleys, with morphology reflecting past and ongoing geomorphic processes and erosion mechanisms (Prasicek et al., 2015). Identifying these different morphologies by topographic analysis is also important to study the development of valleys in relationship with their width.

We noticed in section 3.4 that the wideness index could exhibit patterns than may be characteristic of given landforms, such as glacial cirques in Scotland and fluvial terraces in the Alps.

However, the characterization of valley morphology on a larger scale requires more than their width. Few attempts have been made at characterizing valley morphology from topographic data. Most of these studies focus on the distinctive cross sectional profile of valleys to assess the the glacial impact in valleys (Zimmer and Gabet, 2018; Daxberger et al., 2014; Prasicek et al., 2015), and thus require the extraction and analysis of cross sections, which renders continuous analysis more expensive in term of computing efficiency.

https://doi.org/10.5194/egusphere-2026-3145
Preprint. Discussion started: 15 June 2026

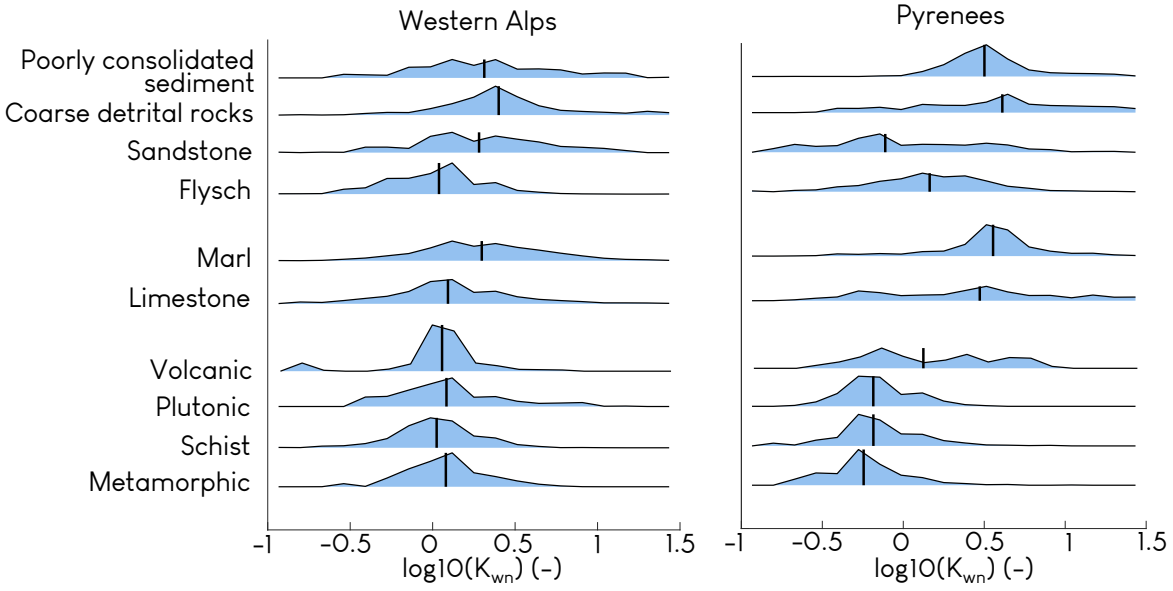

Figure 8. Distribution of the logged valley wideness index as a function of lithology in the Western Alps and Pyrenean Foothills. The vertical bars indicate the median of each distribution.

We took a different approach and analyzed the internal distribution of slope and relative elevation compared to the nearest channel for the valleys obtained with the flooding approach to see if different patterns could be detected. We focus on the flooding method since it does not intrinsically force any slope or elevation limit. We expect different slope and elevation distribution within valleys depending on their morphology, as shown on Figure 9 (Interpretation panel): wide flat valleys are expected to mainly include low slopes and elevations above channels, valleys presenting terraces are expected to have low slopes and high elevations above channels, while narrow, V-shape, confined valleys with steep walls are expected to have higher slopes and various elevations since the geometric method includes a portion of the valley walls in the valley.

In each region, we examine separately the upstream narrow valleys and the downstream wide valleys (see Figure 9). We separate them based on a width threshold of 300 m. The shape of the density pattern varies between regions. As for narrow valleys, the main valleys are dominated by high-slopes and low elevations, except for the Scottish Highlands where slope is lower than the more mountainous regions. The Pyrennean Foothill also have lower slopes than the two others. In the wider valleys, the distribution is dominated by low slopes and various elevations characteristic of the floodplains, and eventual terraces. The Scottish Highlands and Pyrenean Foothill have lower elevations in their distribution.

Furthermore, in the narrow valleys of the Scottish Highlands and Western Alps, a distinctive low-density domain emerges where the slope and elevation seem to be correlated. This could be characteristic of curved valley walls and possibly a signature of glacial modification of the landscapes.

https://doi.org/10.5194/egusphere-2026-3145
Preprint. Discussion started: 15 June 2026

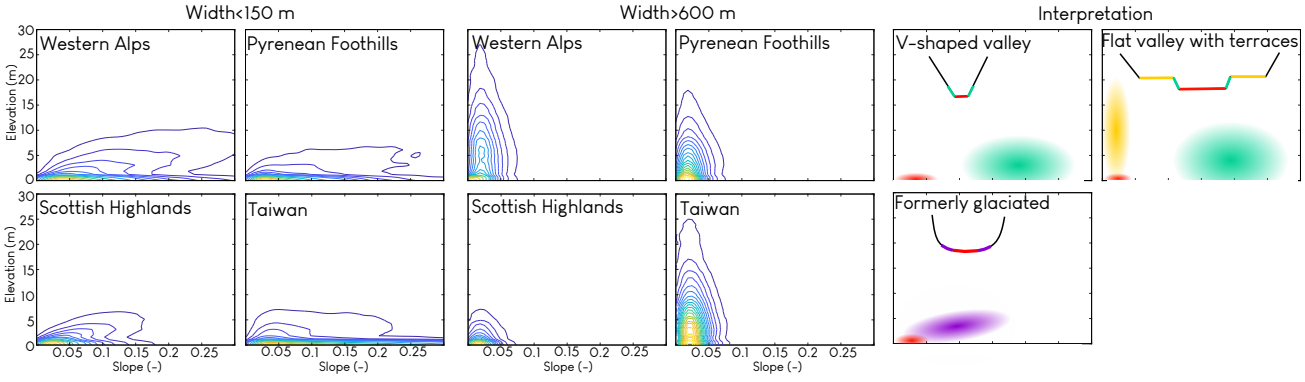

Figure 9. Distribution of slope and elevation above channel in the valleys. Each panel represents the density contours for one region calculated from a 2D histogram of slope and elevation inside valleys and smoothed using a Gaussian filter.

Such analyses could support objective classification of valley types across large regions using DEM-based metrics. In the scope of a global analysis of valley width distribution, the classification of valley morphology could help discriminate between the geomorphic processes involved and thus help refine our knowledge of how these different processes are affected by lithology, climate, and tectonics.

5 Conclusions

This study compared two automated approaches for valley extraction and width measurement from digital elevation models: a geometrical method (Clubb et al., 2022) and a new flooding method based on a simplified hydraulic formalism. Although both methods can be calibrated to achieve similar agreement with mapped alluvial deposits, they differ in sensitivity, computational cost, and conceptual definition of valleys. The geometrical method is more sensitive to parameter selection but offers greater adaptability to local topographic variability and yields valley widths that are independent of drainage area, making it well suited for analyses of valley geometry and width–area scaling. In contrast, the flooding method is more robust to parameter choice and captures hydraulically connected, flood-prone valley extents, but at higher computational cost.

Our results demonstrate that valley width exhibits a robust power-law scaling with drainage area across diverse geomorphic settings, with exponents ranging from 0.2 to 0.6 and most commonly between 0.3 and 0.5. These values are consistent with previous studies and support the interpretation that valley widening is primarily controlled by drainage area.

The wideness index reveals systematic spatial deviations linked to lithology, tectonic structures, and geomorphic history. In particular, resistant rocks are associated with narrower valleys, while weaker materials correspond to wider valleys.

These preliminary results highlight the potential of systematic valley extraction for the study of controls on valley morphology. Characterizing valley wideness and morphology over large spatial scales and linking it to drainage area, climate, tectonics, and lithological metrics might help further our understanding the dynamics of valley erosion and sediment storage in mountain regions.

https://doi.org/10.5194/egusphere-2026-3145
Preprint. Discussion started: 15 June 2026

Code availability. The full codes and workflow will be available in Matlab and Python by the time of publication.

Data availability. Topographic data were retrieved from the NASA Shuttle Radar Topography Mission (2013) (NASA Shuttle Radar Topography Mission (SRTM), 2013)

Author contributions. Fiona Clubb developed the geometrical valley extraction method. Philippe Steer developped the flooding method. Aude Lurin devised the study, ran the analyses and wrote the manuscript with input from Philippe Steer, Fiona Clubb and Boris Gailleton.

Competing interests. The authors have no competing interests related to the work reported in this paper.

https://doi.org/10.5194/egusphere-2026-3145
Preprint. Discussion started: 15 June 2026

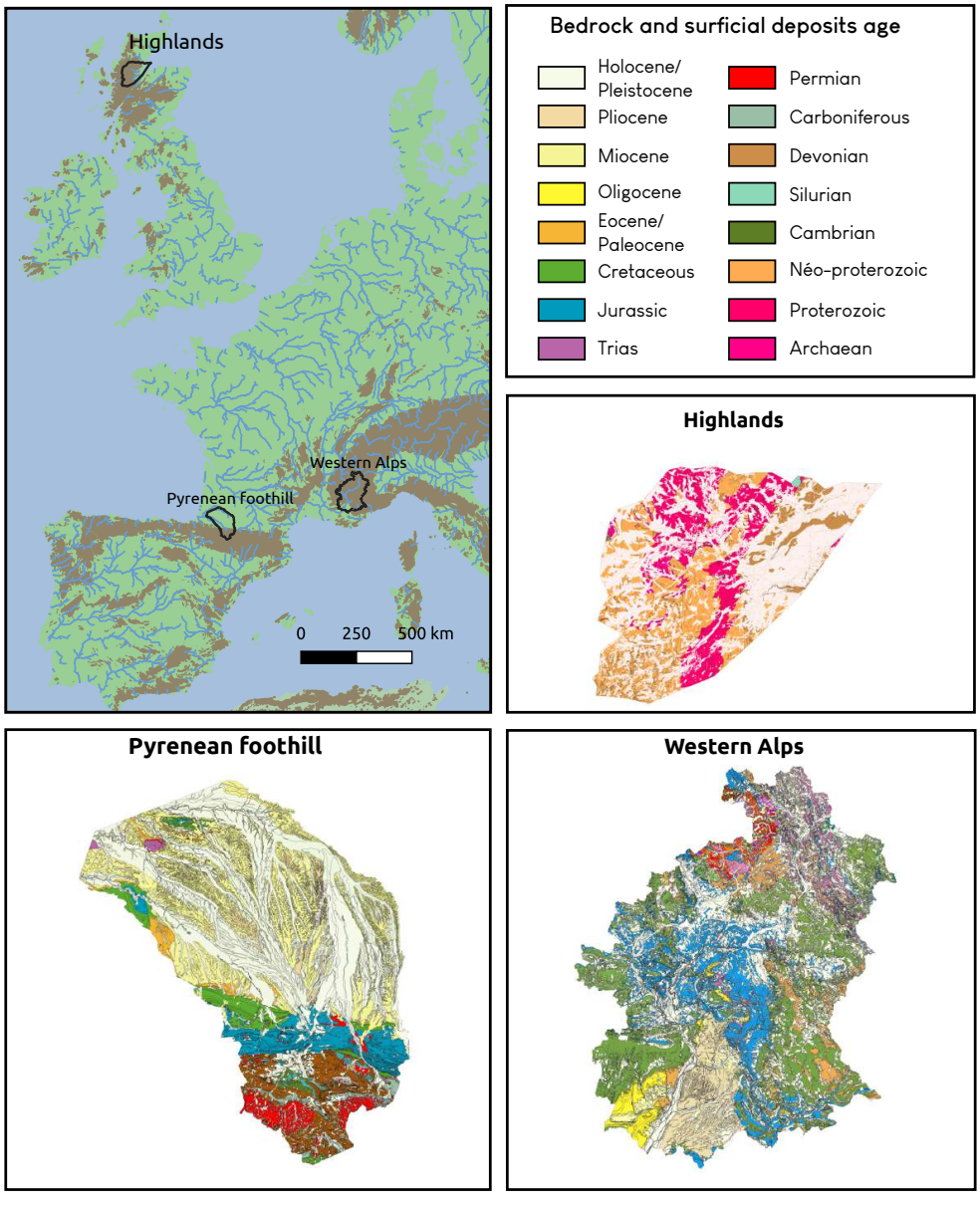

Figure A1. Geological maps for the Western Alps, Pyrenean Foothills and Scottish Highlands regions. The maps were retrieved from national geological surveys.

https://doi.org/10.5194/egusphere-2026-3145
Preprint. Discussion started: 15 June 2026

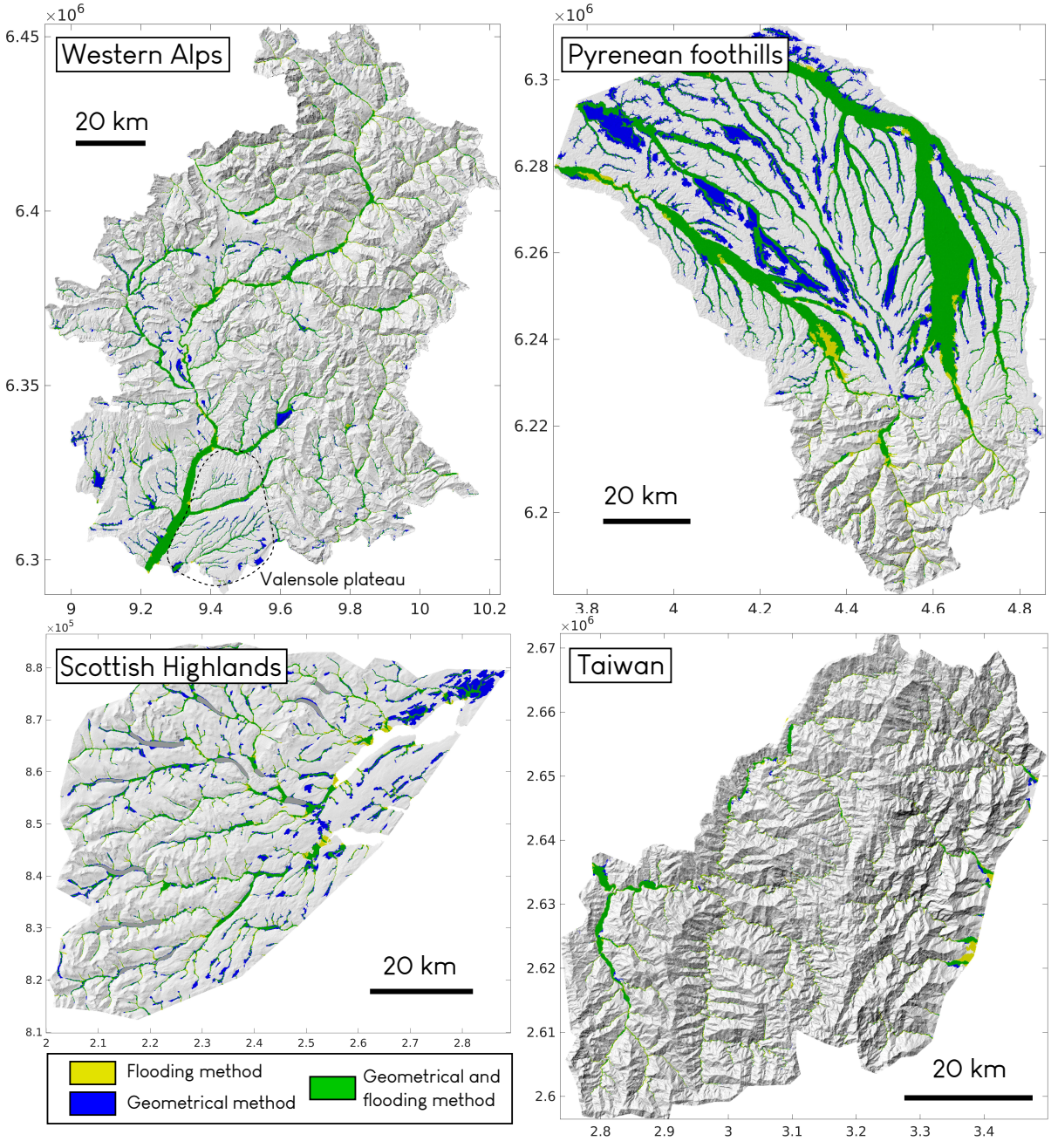

Figure A2. Map of the true positive, false negative and false positive pixels compared with the alluvial deposits for the four areas.

https://doi.org/10.5194/egusphere-2026-3145
Preprint. Discussion started: 15 June 2026

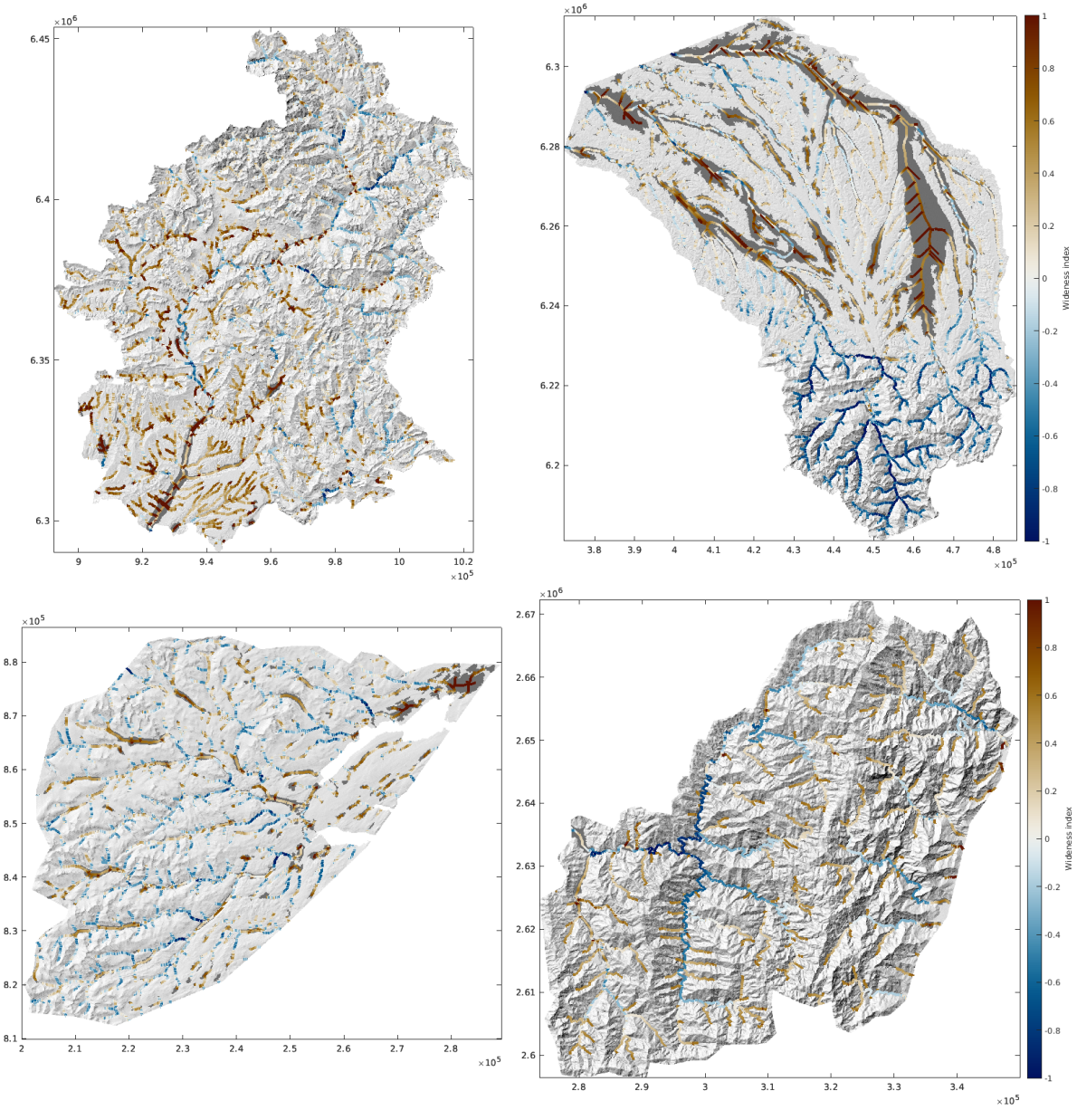

Figure A3. Maps of the wideness index of the valley network for the geometrical method in the four catchement. The Wideness index was logged and normalised to identify the widened and narrowed areas. The grey areas represent the valley masks.

https://doi.org/10.5194/egusphere-2026-3145
Preprint. Discussion started: 15 June 2026

References

Amos, C. and Burbank, D.: Channel width response to differential uplift , J. Geophys. Res., 112(F2), F02 010, https://doi.org/10.1029/2006JF000672, 2007.

Ballantyne, C. K.: After the ice: Holocene geomorphic activity in the Scottish Highlands, Scottish Geographical Journal, 124, 8–52, 2008.

Baynes, E. R., Lague, D., Steer, P., Bonnet, S., and Illien, L.: Sediment flux-driven channel geometry adjustment of bedrock and mixed gravel-bedrock rivers, Earth Surf. Proc. Land., https://doi.org/10.1002/esp.4996, 2020.

Baynes, E. R., Lague, D., Steer, P., and Davy, P.: Dynamic bedrock channel width during knickpoint retreat enhances undercutting of coupled hillslopes, Earth Surface Processes and Landforms, 47, 3629–3640, 2022.

Beer, A. R., Turowski, J. M., and Kirchner, J. W.: Spatial patterns of erosion in a bedrock gorge, J. Geophys. Res. Earth Surface, 122, 191–214, https://doi.org/10.1002/2016JF003850, 2017.

Beeson, H. W., Flitcroft, R. L., Fonstad, M. A., and Roering, J. J.: Deep-seated landslides drive variability in valley width and increase connectivity of salmon habitat in the Oregon Coast Range, JAWRA Journal of the American Water Resources Association, 54, 1325–1340, 2018.

Bernard, M., Steer, P., Gallagher, K., and Egholm, D. L.: The impact of lithology on fjord morphology, Geophysical Research Letters, 48, e2021GL093 101, 2021.

Bickerdike, H., Evans, D., Stokes, C., and Ó Cofaigh, C.: The glacial geomorphology of the Loch Lomond (Younger Dryas) Stadial in Britain: a review, Journal of Quaternary Science, 33, 1–54, 2018.

Bradley, D. N. and Tucker, G. E.: The storage time, age, and erosion hazard of laterally accreted sediment on the floodplain of a simulated meandering river, J. Geophys. Res. Earth Surface, 118, 1308–1319, https://doi.org/10.1002/jgrf.20083, 2013.

Brocard, G. and der Beek, P. V.: Influence of incision rate, rock strength and bedload supply on bedrock river gradients and valley-flat widths: Field-based evidence and calibrations from western Alpine rivers (SE France), in: Tectonics, Climate and Landscape Evolution, edited by S.D. Willett and N. Hovius and M.T. Brandon and D. Fisher, Geol. Soc. Am. Spec. Publ., 2006.

Brook, M. S., Purdie, H. L., and Crow, T. V.: Valley cross-profile morphology and glaciation in Park Valley, Tararua Range, New Zealand, Journal of the Royal Society of New Zealand, 35, 399–407, 2005.

Brunner, G. W.: HEC-RAS river analysis system user's manual version 5.0, US Army Corps of Engineers, 962, 2016.

Bufe, A., Paola, C., and Burbank, D. W.: Fluvial bevelling of topography controlled by lateral channel mobility and uplift rate, Nature Geoscience, 9, 706, 2016.

Capote, R., Muñoz, J. A., Simón, J. L., Liesa, C. L., and Arlegui, L. E.: Alpine tectonics I: the Alpine system north of the Betic Cordillera, 2002.

Champagnac, J., Molnar, P., Anderson, R., Sue, C., and Delacou, B.: Quaternary erosion-induced isostatic rebound in the western Alps, Geology, 35, 195–198, https://doi.org/10.1130/G23053A.1, 2007.

Chen, C.-S. and Chen, Y.-L.: The rainfall characteristics of Taiwan, Monthly Weather Review, 131, 1323–1341, 2003.

Cheng, J., Huang, Y., Wu, H., Yeh, J., and Chang, C.: Hydrometeorological and landuse attributes of debris flows and debris floods during typhoon Toraji, July 29–30, 2001 in central Taiwan, Journal of hydrology, 306, 161–173, 2005.

Clark, C. D., Ely, J. C., Hindmarsh, R. C., Bradley, S., Ignéczi, A., Fabel, D., Ó Cofaigh, C., Chiverrell, R. C., Scourse, J., Benetti, S., et al.: Growth and retreat of the last British–Irish Ice Sheet, 31 000 to 15 000 years ago: the BRITICE-CHRONO reconstruction, Boreas, 51, 699–758, 2022.

https://doi.org/10.5194/egusphere-2026-3145
Preprint. Discussion started: 15 June 2026

Clubb, F. J., Mudd, S. M., Milodowski, D. T., Hurst, M. D., and Slater, L. J.: Objective extraction of channel heads from high-resolution topographic data, Water Resources Research, 50, 4283–4304, 2014.

Clubb, F. J., Mudd, S. M., Milodowski, D. T., Valters, D. A., Slater, L. J., Hurst, M. D., and Limaye, A. B.: Geomorphometric delineation of floodplains and terraces from objectively defined topographic thresholds, Earth Surface Dynamics, 5, 369–385, 2017.

Clubb, F. J., Weir, E. F., and Mudd, S. M.: Continuous measurements of valley floor width in mountainous landscapes, Earth Surface Dynamics, 10, 437–456, 2022.

Clubb, F. J., Mudd, S. M., Schildgen, T. F., van der Beek, P. A., Devrani, R., and Sinclair, H. D.: Himalayan valley-floor widths controlled by tectonically driven exhumation, Nature Geoscience, 16, 739–746, 2023.

Constantine, J. A., Dunne, T., Ahmed, J., Legleiter, C., and Lazarus, E. D.: Sediment supply as a driver of river meandering and floodplain evolution in the Amazon Basin, Nature Geoscience, 7, 899, 2014.

Cooper, D. J., Andersen, D. C., and Chimner, R. A.: Multiple pathways for woody plant establishment on floodplains at local to regional scales, Journal of Ecology, 91, 182–196, 2003.

Cossart, E., Braucher, R., Fort, M., Bourlès, D., and Carcaillet, J.: Slope instability in relation to glacial debuttressing in alpine areas (Upper Durance catchment, southeastern France): Evidence from field data and 10Be cosmic ray exposure ages, Geomorphology, 95, 3–26, 2008.

Curry, M. E. and van der Beek, P.: Exploring Controls on Post-Orogenic Topographic Stasis of the Pyrenees Mountains With Inverse Landscape Evolution Modeling, Journal of Geophysical Research: Earth Surface, 130, e2024JF007759, https://doi.org/https://doi.org/10.1029/2024JF007759, e2024JF007759 2024JF007759, 2025.

Dahlquist, M. P. and West, A. J.: The imprint of erosion by glacial lake outburst floods in the topography of central Himalayan rivers, Earth Surface Dynamics, 10, 705–722, 2022.

Davidson, S. L., Marin-Esteve, B., and Eaton, B.: What controls river widening? Comparing large and extreme flood events, Earth Surface Processes and Landforms, 49, 3046–3062, 2024.

Davy, P. and Lague, D.: The erosion / transport equation of landscape evolution models revisited, J. Geophys. Res., 114, https://doi.org/10.1029/2008JF001146, 2009.

Daxberger, H., Dalumpines, R., Scott, D. M., and Riller, U.: The ValleyMorph Tool: An automated extraction tool for transverse topographic symmetry (T-) factor and valley width to valley height (Vf-) ratio, Computers & Geosciences, 70, 154–163, 2014.

Degiorgis, M., Gnecco, G., Gorni, S., Roth, G., Sanguineti, M., and Taramasso, A. C.: Classifiers for the detection of flood-prone areas using remote sensed elevation data, Journal of hydrology, 470, 302–315, 2012.

Dunne, T., Constantine, J. A., and Singer, M.: The Role of Sediment Transport and Sediment Supply in the Evolution of River Channel and Floodplain Complexit, Transactions, Japanese Geomorphological Union, 31, 155–170, 2010.

Farr, T. G. and Chadwick, O. A.: Geomorphic processes and remote sensing signatures of alluvial fans in the Kun Lu Mountains, China, J. Geophys. Res., 101, 23,091–23,100, 1996.

Farr, T. G., Rosen, P. A., Caro, E., Crippen, R., Duren, R., Hensley, S., Kobrick, M., Paller, M., Rodriguez, E., Roth, L., et al.: The shuttle radar topography mission, Reviews of geophysics, 45, https://doi.org/10.1029/2005RG000183, 2007.

Felipe-Lucia, M. R., Comín, F. A., and Bennett, E. M.: Interactions among ecosystem services across land uses in a floodplain agroecosystem, Ecology and society, 19, 2014.

Finnegan, N. J. and Dietrich, W. E.: Episodic bedrock strath terrace formation due to meander migration and cutoff, Geology, 39, 143–146, https://doi.org/10.1130/G31716.1, 2011.

https://doi.org/10.5194/egusphere-2026-3145
Preprint. Discussion started: 15 June 2026

Fisher, G. B., Bookhagen, B., and Amos, C. B.: Channel planform geometry and slopes from freely available high-spatial resolution imagery and DEM fusion: Implications for channel width scalings, erosion proxies, and fluvial signatures in tectonically active landscapes, Geomorphology, 194, 46–56, 2013.

Ford, M., Hemmer, L., Vacherat, A., Gallagher, K., and Christophoul, F.: Retro-wedge foreland basin evolution along the ECORS line, eastern Pyrenees, France, Journal of the Geological Society, 173, 419–437, 2016.

Gailleton, B., Steer, P., Davy, P., Schwanghart, W., and Bernard, T.: GraphFlood 1.0: an efficient algorithm to approximate 2D hydrodynamics for landscape evolution models, Earth Surface Dynamics, 12, 1295–1313, 2024.

Gilbert, G.: Report on the Geology of the Henry Mountains U.S. Geographical and Geological Survey of the Rocky Mountain Region Washington D.C, Tech. rep., 1877.

Godard, V., Hippolyte, J.-C., Cushing, E., Espurt, N., Fleury, J., Bellier, O., Ollivier, V., and Team, t. A.: Hillslope denudation and morphologic response to a rock uplift gradient, Earth Surface Dynamics, 8, 221–243, https://doi.org/https://doi.org/10.5194/esurf-8-221-2020, 2020.

Groeber, O. H. and Langston, A. L.: The role of Talus pile mobility in valley widening processes and the development of wide bedrock valleys, Buffalo River, AR, Journal of Geophysical Research: Earth Surface, 129, e2023JF007 612, 2024.

Gupta, S., Collier, J. S., Palmer-Felgate, A., and Potter, G.: Catastrophic flooding origin of shelf valley systems in the English Channel, Nature, 448, 342–345, 2007.

Hancock, G. S. and Anderson, R. S.: Numerical modeling of fluvial strath-terrace formation in response to oscillating climate, Geol. Soc. Am. Bull., 114, 1131–1142, 2002.

Harel, E., Goren, L., Crouvi, O., Ginat, H., and Shelef, E.: Drainage reorganization induces deviations in the scaling between valley width and drainage area, Earth Surface Dynamics, 10, 875–894, 2022.

Horton, R. E.: Erosional development of streams and their drainage basins; hydrophysical approach to quantitative morphology, Geological society of America bulletin, 56, 275–370, 1945.

Kearney, W., Schwanghart, W., Lamprecht, A.-L., Scherler, D., Bringezu, T., Bartha, D., and Gailleton, B.: TopoToolbox 3-a laboratory for topographic analysis, in: EGU General Assembly Conference Abstracts, pp. EGU25–8678, 2025.

Keen-Zebert, A., Hudson, M. R., Shepherd, S. L., and Thaler, E. A.: The effect of lithology on valley width, terrace distribution, and bedload provenance in a tectonically stable catchment with flat-lying stratigraphy, Earth Surface Processes and Landforms, 42, 1573–1587, 2017.

Kirby, E. and Whipple, K. X.: Quantifying differential rock-uplift rates via stream profile analysis, Geology, 29, 415–418, 2001.

Lacan, P. and Ortuño Candela, M.: Active Tectonics of the Pyrenees: A review., Journal Of Iberian Geology, 2012, vol. 38, num. 1, p. 9-30, 2012.

Lague, D.: The stream power river incision model: evidence, theory and beyond, Earth Surface Processes and Landforms, 39, 38–61, https://doi.org/10.1002/esp.3462, _eprint: https://onlinelibrary.wiley.com/doi/pdf/10.1002/esp.3462, 2014.

Lancaster, S. T.: Evolution of sediment accommodation space in steady state bedrock-incising valleys subject to episodic aggradation, Journal of Geophysical Research: Earth Surface, 113, 2008.

Langston, A. L. and Temme, A. J. A. M.: Bedrock erosion and changes in bed sediment lithology in response to an extreme flood event: The 2013 Colorado Front Range flood, Geomorphology, 328, 1–14, https://doi.org/10.1016/j.geomorph.2018.11.015, 2019.

Langston, A. L. and Tucker, G. E.: Developing and exploring a theory for the lateral erosion of bedrock channels for use in landscape evolution models, Earth Surface Dynamics, 6, 1–27, https://doi.org/10.5194/esurf-6-1-2018, 2018.

https://doi.org/10.5194/egusphere-2026-3145
Preprint. Discussion started: 15 June 2026

Lavé, J. and Avouac, J.-P.: Active dolding of fluvial terraces across the Siwaliks Hills, himalayas of central Nepal, J. Geophys. Res., 105-B3, 5735–5770, 2000.

Lavé, J. and Avouac, J.-P.: Fluvial incision and tectonic uplift across the Himalayas of central Nepal, J. Geophys. Res., 106-B11, 26,561–26,591, 2001.

Leopold, L. B. and Maddock, T. J.: The hydrolic geometry of stream channels and some physiographic implications, U. S. Geol. Survey. Professional Paper, 252, 57, 1953.

Li, Y., Liu, G., and Cui, Z.: Glacial valley cross-profile morphology, Tian Shan Mountains, China, Geomorphology, 38, 153–166, 2001.

Lin, M. and Jeng, F.: Characteristics of hazards induced by extremely heavy rainfall in Central Taiwan—Typhoon Herb, Engineering Geology, 58, 191–207, 2000.

Lóczy, D., Kis, É., and Schweitzer, F.: Local flood hazards assessed from channel morphometry along the Tisza River in Hungary, Geomorphology, 113, 200–209, 2009.

Maddy, D., Bridgland, D., and Westaway, R.: Uplift-driven valley incision and climate-controlled river terrace development in the Thames Valley, UK, Quaternary International, 79, 23–36, 2001.

Malatesta, L., Prancevic, J., and Avouac, J.-P.: Autogenic entrenchment patterns and terraces due to coupling with lateral erosion in incising alluvial channels, J. Geophys. Res. Earth Surface, 122, 335–355, https://doi.org/10.1002/2015JF003797, 2017.

May, C., Roering, J., Eaton, L., and Burnett, K.: Controls on valley width in mountainous landscapes: The role of landsliding and implications for salmonid habitat, Geology, 41, 503–506, 2013.

McGee, W.: Glacial canons, The Journal of Geology, 2, 350–364, 1894.

Montgomery, D. R. and Dietrich, W. E.: Channel initiation and the problem of landscape scale, Science, 255, 826–830, 1992.

NASA Shuttle Radar Topography Mission (SRTM): Shuttle Radar Topography Mission (SRTM) Global, https://doi.org/10.5069/G9445JDF, 2013.

Nobre, A. D., Cuartas, L. A., Hodnett, M., Rennó, C. D., Rodrigues, G., Silveira, A., and Saleska, S.: Height Above the Nearest Drainage–a hydrologically relevant new terrain model, Journal of Hydrology, 404, 13–29, 2011.

Noman, N. S., Nelson, E. J., and Zundel, A. K.: Improved process for floodplain delineation from digital terrain models, Journal of water resources planning and management, 129, 427–436, 2003.

Passalacqua, P., Do Trung, T., Foufoula-Georgiou, E., Sapiro, G., and Dietrich, W. E.: A geometric framework for channel network extraction from lidar: Nonlinear diffusion and geodesic paths, Journal of Geophysical Research: Earth Surface, 115, 2010.

Peng, T.-H., Li, Y.-H., and Wu, F. T.: Tectonic uplift rates of the Taiwan island since the early Holocene, Mem. Geol. Soc. China, 2, 57–69, 1977.

Pons, F., Hocini, N., and Garambois, P.-A.: Cartino2D: Scalable and Automated 2D Shallow Water Rainfall-Flood Inundation Modeling up to Very High Resolution for Large Domains, EGUsphere, 2026, 1–41, 2026.

Prasicek, G., Larsen, I. J., and Montgomery, D. R.: Tectonic control on the persistence of glacially sculpted topography, Nature communications, 6, 8028, 2015.

Rockwell, T., Keller, E., Clark, M., and Johnson, D.: Chronology and rates of faulting of Ventura River terraces, California, Geol. Soc. Am. Bull., 95, 1466–1474, 1984.

Roest, W. and Srivastava, S.: Kinematics of the plate boundaries between Eurasia, Iberia, and Africa in the North Atlantic from the Late Cretaceous to the present, Geology, 19, 613–616, 1991.

https://doi.org/10.5194/egusphere-2026-3145
Preprint. Discussion started: 15 June 2026

Rosenbaum, G., Lister, G. S., and Duboz, C.: Relative motions of Africa, Iberia and Europe during Alpine orogeny, Tectonophysics, 359, 117–129, 2002.

Rougier, G., Ford, M., Christophoul, F., and Bader, A.-G.: Stratigraphic and tectonic studies in the central Aquitaine Basin, northern Pyrenees: Constraints on the subsidence and deformation history of a retro-foreland basin, Comptes Rendus. Géoscience, 348, 224–235, 2016.

Sampson, C. C., Smith, A. M., Bates, P. D., Neal, J. C., Alfieri, L., and Freer, J. E.: A high-resolution global flood hazard model, Water resources research, 51, 7358–7381, 2015.

Schanz, S. A. and Montgomery, D. R.: Lithologic controls on valley width and strath terrace formation, Geomorphology, 258, 58–68, https://doi.org/10.1016/j.geomorph.2016.01.015, 2016.

Schanz, S. A. and Montgomery, D. R.: Lithologic controls on valley width and strath terrace formation, Geomorphology, 258, 58–68, 2016.

Schmid, S., Fügenschuh, B., Kissling, E., and Schuster, R.: Tectonic map and overall architecture of the Alpine orogen, Eclogae Geologicae Helvetiae, 97, 93–117, https://doi.org/10.1007/s00015-004-1113-x, 2004.

Schumm, S. A. and Ethridge, F. G.: Origin, evolution and morphology of fluvial valleys, 1994.

Schwanghart, W. and Scherler, D.: TopoToolbox 2 – MATLAB-based Software for Topographic Analysis and Modeling in Earth Surface Sciences, Earth Surface Dynamics, 2, 1–7, https://doi.org/10.5194/esurf-2-1-2014, 2014.

Schwanghart, W. and Scherler, D.: Bumps in river profiles: uncertainty assessment and smoothing using quantile regression techniques, Earth Surface Dynamics, 5, 821–839, 2017.

Seno, T.: The instantaneous rotation vector of the Philippine Sea plate relative to the Eurasian plate, Tectonophysics, 42, 209–226, 1977.

Snyder, N. P., Whipple, K. X., Tucker, G. E., and Merritts, D. J.: Channel response to tectonic forcing: analysis of stream morphology and hydrology in the Mendocino triple junction region, northern California, Geomorphology, 53, 97–127, 2003.

Stoffel, M., Wyżga, B., and Marston, R. A.: Floods in mountain environments: A synthesis, Geomorphology, 272, 1–9, 2016.

Stout, J. C. and Belmont, P.: TerEx Toolbox for semi-automated selection of fluvial terrace and floodplain features from lidar, Earth Surface Processes and Landforms, 39, 569–580, 2014.

Suppe, J.: Kinematics of arc-continent collision, flipping of subduction and back-arc spreading near Taiwan, 1984.

Thorp, J. H., Thoms, M. C., and Delong, M. D.: The riverine ecosystem synthesis: biocomplexity in river networks across space and time, River Research and Applications, 22, 123–147, 2006.

Thorp, J. H., Thoms, M. C., and Delong, M. D.: The riverine ecosystem synthesis: toward conceptual cohesiveness in river science, Elsevier, 2010.

Tockner, K. and Stanford, J. A.: Riverine flood plains: present state and future trends, Environmental conservation, 29, 308–330, 2002.

Tofelde, S., Bufe, A., and Turowski, J. M.: Hillslope Sediment Supply Limits Alluvial Valley Width, AGU Advances, 3, e2021AV000 641, https://doi.org/https://doi.org/10.1029/2021AV000641, e2021AV000641 2021AV000641, 2022.

Tomkin, J., Brandon, M. T., Pazzaglia, F. J., Barbour, J. R., and Willet, S. D.: Quantitative testing of bedrock incision models for the Clearwater River, NW Washington State, J. Geophys. Res., 108-B6, 2308, https://doi.org/10.1029/2001JB000862, 2003.

Tomscha, S. A., Gergel, S. E., and Tomlinson, M. J.: The spatial organization of ecosystem services in river-floodplains, Ecosphere, 8, e01 728, 2017.

Turowski, J., Hovius, N., Meng-Long, H., Lague, D., and Men-Chiang, C.: Distribution of erosion across bedrock channels, Earth Surf. Proc. Land., https://doi.org/10.1002/esp.1559, 2007.

Turowski, J. M., Bufe, A., and Tofelde, S.: A physics-based model for fluvial valley width, Earth Surface Dynamics, 12, 493–514, 2024.

Vissers, R. and Meijer, P. T.: Iberian plate kinematics and Alpine collision in the Pyrenees, Earth-Science Reviews, 114, 61–83, 2012.

https://doi.org/10.5194/egusphere-2026-3145
Preprint. Discussion started: 15 June 2026

Whipple, K. X.: Bedrock rivers and the Geomorphology of active orogens, Annual Review of Earth and Planetary Sciences, 32, 151–185, 2004.

Whipple, K. X. and Tucker, G. E.: Dynamics of the stream-power river incision model: Implications for height limits of mountain ranges, landscape response timescales, and research needs, Journal of Geophysical Research: Solid Earth, 104, 17 661–17 674, https://doi.org/10.1029/1999JB900120, _eprint: https://onlinelibrary.wiley.com/doi/pdf/10.1029/1999JB900120, 1999.

Whipple, K. X., Hancock, G. S., and Anderson, R. S.: River incision into bedrock: Mechanics and relative efficacy of plucking, abrasion, and cavitation, GSA Bulletin, 112, 490–503, https://doi.org/10.1130/0016-7606(2000)112<490:RIIBMA>2.0.CO;2, 2000.

Willett, S. D., Fisher, D., Fuller, C., En-Chao, Y., and Chia-Yu, L.: Erosion rates and orogenic-wedge kinematics in Taiwan inferred from fission-track thermochronometry, Geology, 31, 945–948, 2003.

Williams, W. A., Jensen, M. E., Winne, J. C., and Redmond, R. L.: An automated technique for delineating and characterizing valley-bottom settings, Environmental monitoring and assessment, 64, 105–114, 2000.

Yanites, B. J., Mitchell, N. A., Bregy, J. C., Carlson, G. A., Cataldo, K., Holahan, M., Johnston, G. H., Nelson, A., Valenza, J., and Wanker, M.: Landslides control the spatial and temporal variation of channel width in southern Taiwan: Implications for landscape evolution and cascading hazards in steep, tectonically active landscapes, Earth Surface Processes and Landforms, 43, 1782–1797, 2018.

Yi-Ben, T.: Seismotectonics of Taiwan, Tectonophysics, 125, 17–37, 1986.

Zavala, V., Carretier, S., Regard, V., Bonnet, S., Riquelme, R., and Choy, S.: Along-stream variations in valley flank erosion rates measured using 10Be concentrations in colluvial deposits from canyons in the Atacama Desert, Geophysical Research Letters, 48, e2020GL089 961, 2021.

Zhao, Y., Wu, P., Li, J., Lin, Q., and Lu, Y.: A new algorithm for the automatic extraction of valley floor width, Geomorphology, 335, 37–47, 2019.

Zimmer, P. D. and Gabet, E. J.: Assessing glacial modification of bedrock valleys using a novel approach, Geomorphology, 318, 336–347, 2018.

Zwart, H. J.: The geology of the Central Pyrenees, Leidse Geologische Mededelingen, 50, 1–74, 1979.